Supplementary Information for

Summertime low clouds mediate the impact of the large-scale circulation on Arctic sea ice

Yiyi Huang[1], Qinghua Ding[2*], Xiquan Dong[1], Baike Xi[1] and Ian Baxter[2]

[1]Department of Hydrology and Atmospheric Sciences, University of Arizona, Tucson, Arizona, USA

[2]Department of Geography, and Earth Research Institute, University of California, Santa Barbara, Santa Barbara, California, USA

**Corresponding author address:* Dr. Qinghua Ding, Department of Geography, and Earth Research Institute, University of California, Santa Barbara, Santa Barbara, California, USA. Email: qinghua@ucsb.edu; Phone: (805) 893-2309

Supplementary Tables

Supplementary Table 1. Description of Community Earth System Model (CESM) nudging experiments. All simulations are run with CESM1.2.2.1. The Community Atmosphere Model version 5 (CAM5) has a horizontal resolution of 1.25° longitude by 0.9° latitude and 30 vertical levels. The ocean and sea ice models use the displaced pole gx1v6 grid. Greenhouse gas concentrations are prescribed using year 2000 climatological values. Note that the verticla levels are in model's hybrid sigma pressure coordinate.

Experiment	Initial conditions	Wind fields from ERA-Interim	Vertical levels for nudging	The length of simulation	Rationale
Exp-1	Default initial condition from B2000	U,V during 1979-2016	860 hPa above	38 years (1979-2016)	To examine the stability of the nudging runs; The simulations during the 1979-1999 are considered as "spin-up", thus being discarded from the analysis.
Exp-2	Default initial condition from B2000	U,V during 1979-2016	All levels		
Exp-3	Year 2000 from CESM-LE BTR20 member 23 (large sea ice area)	U,V during 1979-2016	860 hPa above		
Exp-4	Year 2000 from CESM-LE BTR20 member 22 (small sea ice area)	U,V during 1979-2016	860 hPa above		
Exp-5	Year 2000 from CESM-LE BTR20 member 23 (large sea ice area)	U,V during 2000-2016	860 hPa above	17 years (2000-2016)	To examine the impacts of summertime large-scale atmospheric circulation on cloud, radiation and sea ice with different initial conditions; No "spin-up" for this sets of simulations
Exp-6	Year 2000 from CESM-LE BTR20 member 22 (small sea ice area)	U,V during 2000-2016	860 hPa above		
Exp-7	Year 2000 from CESM-LE BTR20 member 14 (thick sea ice)	U,V during 2000-2016	860 hPa above		
Exp-8	Year 2000 from CESM-LE BTR20 member 20 (thin sea ice)	U,V during 2000-2016	860 hPa above		

Supplementary Figures

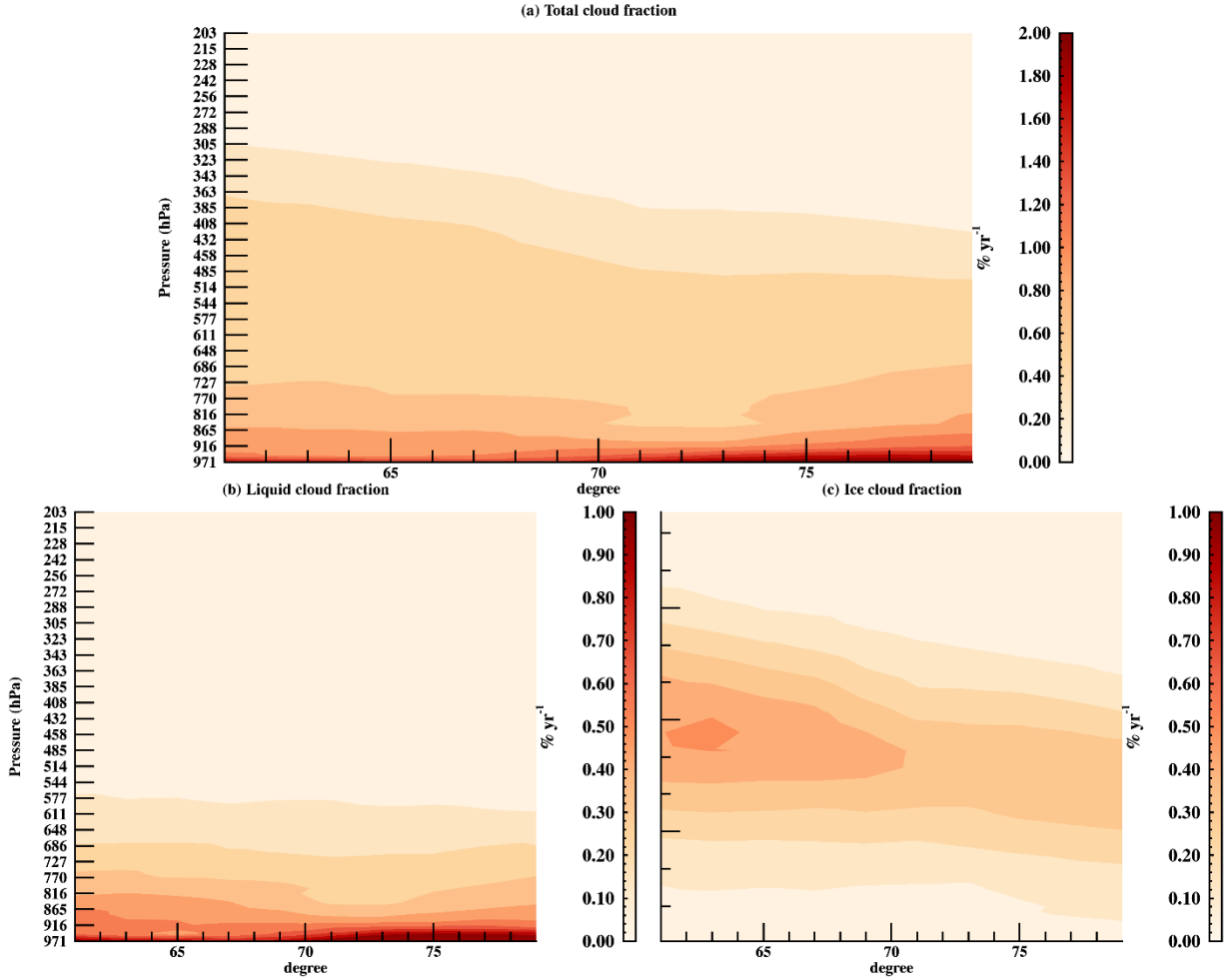

Supplementary Figure 1. Linear trend of cloud fraction as a function of height and latitude for (a) total cloud fraction, (b) liquid cloud fraction and (c) ice cloud fraction from the Global Climate Model (GCM) Oriented Cloud-Aerosol Lidar and Infrared Pathfinder Satellite Observation (CALIPSO) Cloud Product (CALIPSO-GOCCP) during 2006-2016.

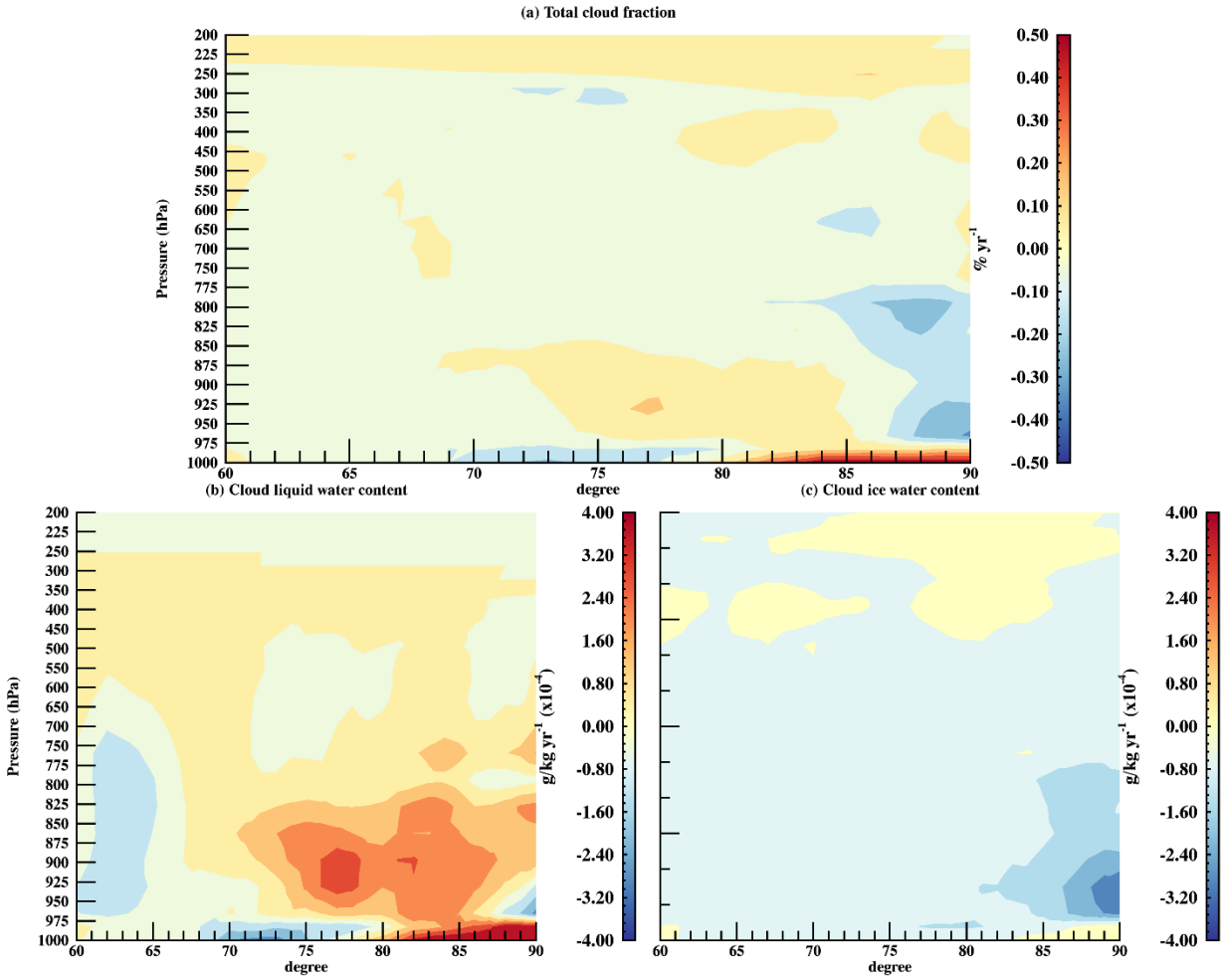

Supplementary Figure 2. Same as Supplementary Figure 1, but using data from ERA-Interim reanalysis during 2000-2016.

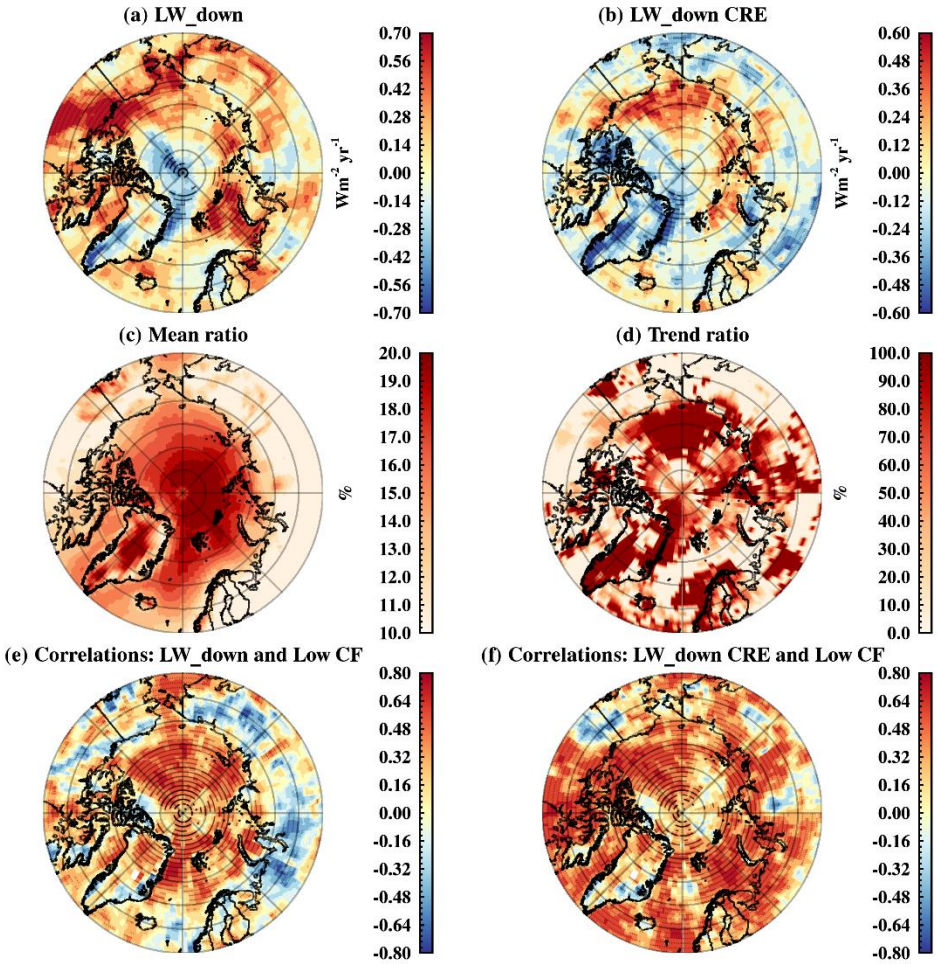

Supplementary Figure 3. Linear trend of JJA (a) downwelling longwave (LW_down) flux and (b) LW_down cloud radiative effect (CRE) at the surface during 2000-2016 in CERES-EBAF Ed4.0 satellite product. The ratio between (c) climatological mean LW_down CRE relative to LW_down flux as well as (d) linear trend of LW_down CRE relative to LW_down flux. (e) The correlations between LW_down flux and low cloud fraction (CF) using linearly detrended data. (f) The correlations between LW_down CRE and low cloud fraction (CF) using linearly detrended data

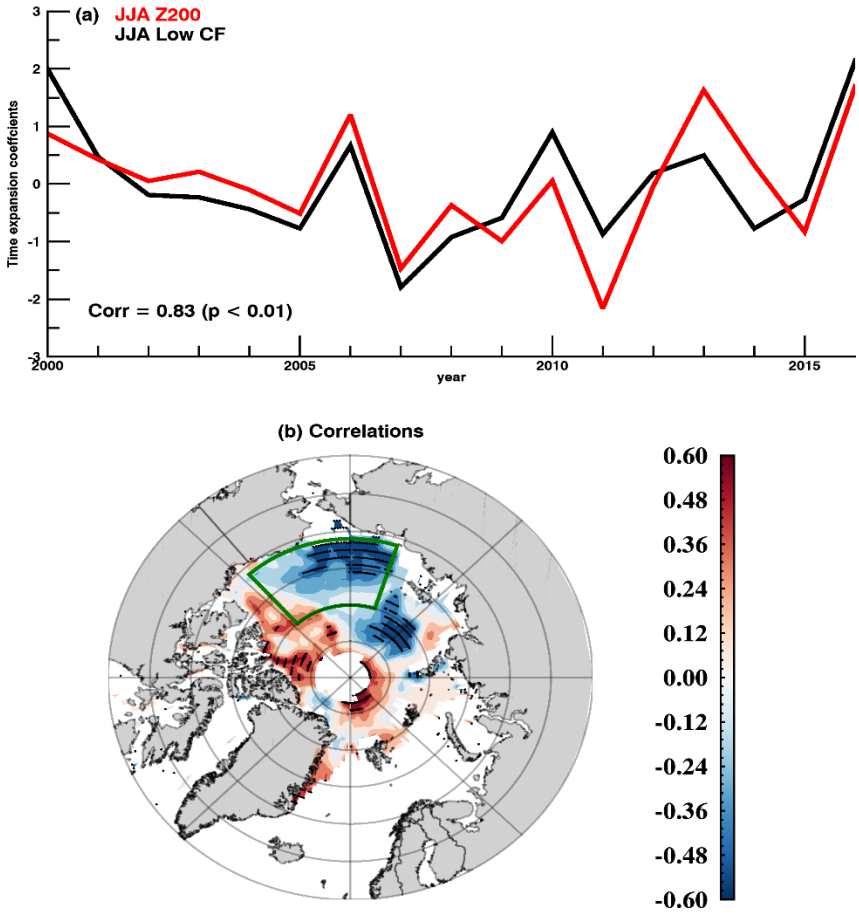

Supplementary Figure 4. Same as Supplementary Figures 1f and 1g, but using detrended data.

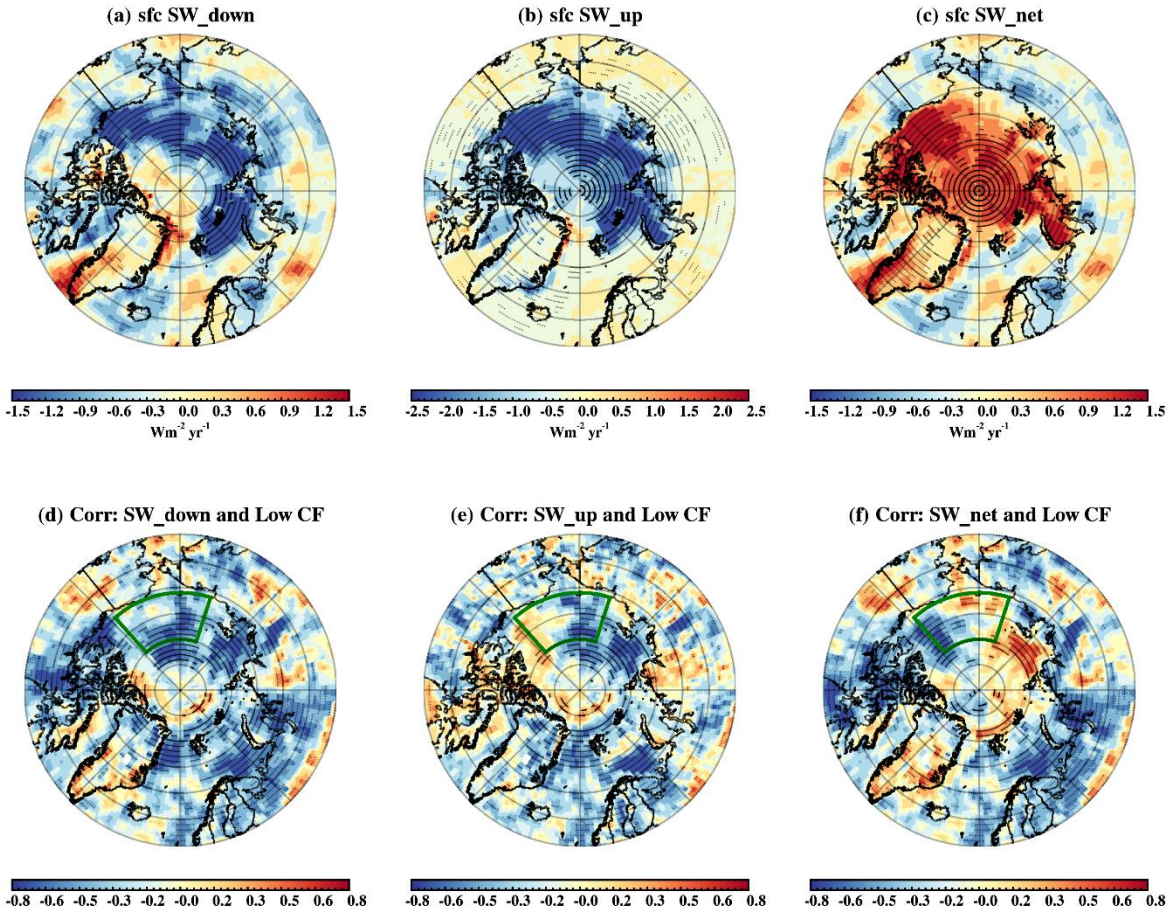

Supplementary Figure 5. Linear trend of JJA (a) downwelling shortwave (SW_down) flux, (b) upwelling shortwave (SW_up) flux, and (b) net shortwave (SW_net) flux at the surface during 2000-2016 in CERES-EBAF Ed4.0 satellite product. (d) Correlations between detrended JJA SW_down flux and low cloud fraction (CF) (e) Correlations between detrended JJA SW_up flux and low CF. (f) Correlations between detrended JJA SW_net flux and low CF.

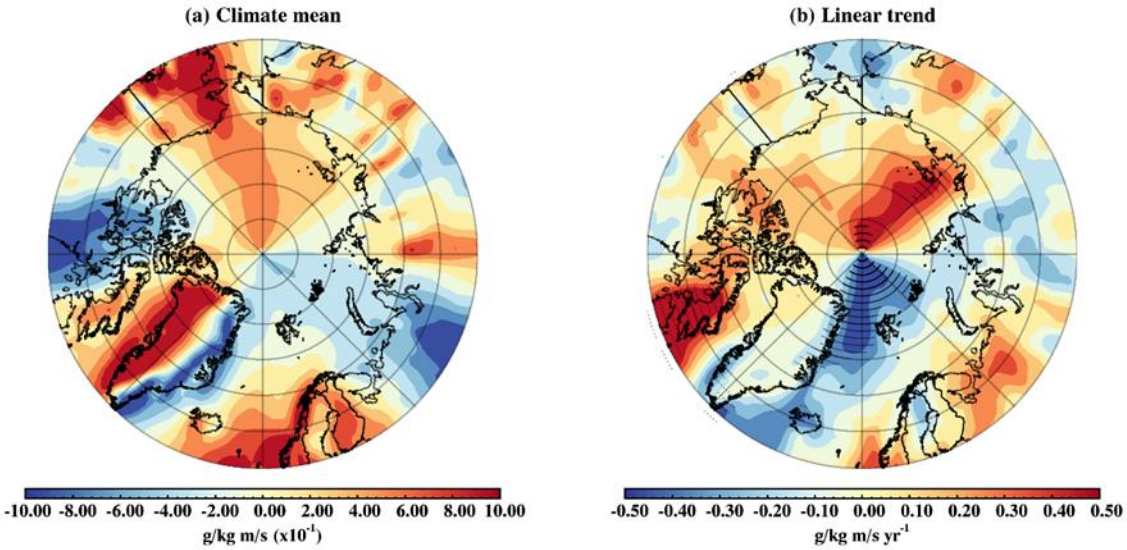

Supplementary Figure 6. (a) The JJA average meridional moisture transport (vq) at 950 hPa. (b)The linear trend of JJA meridional moisture transport at 950 hPa during 2000-2016 in ERA-Interim reanalysis.

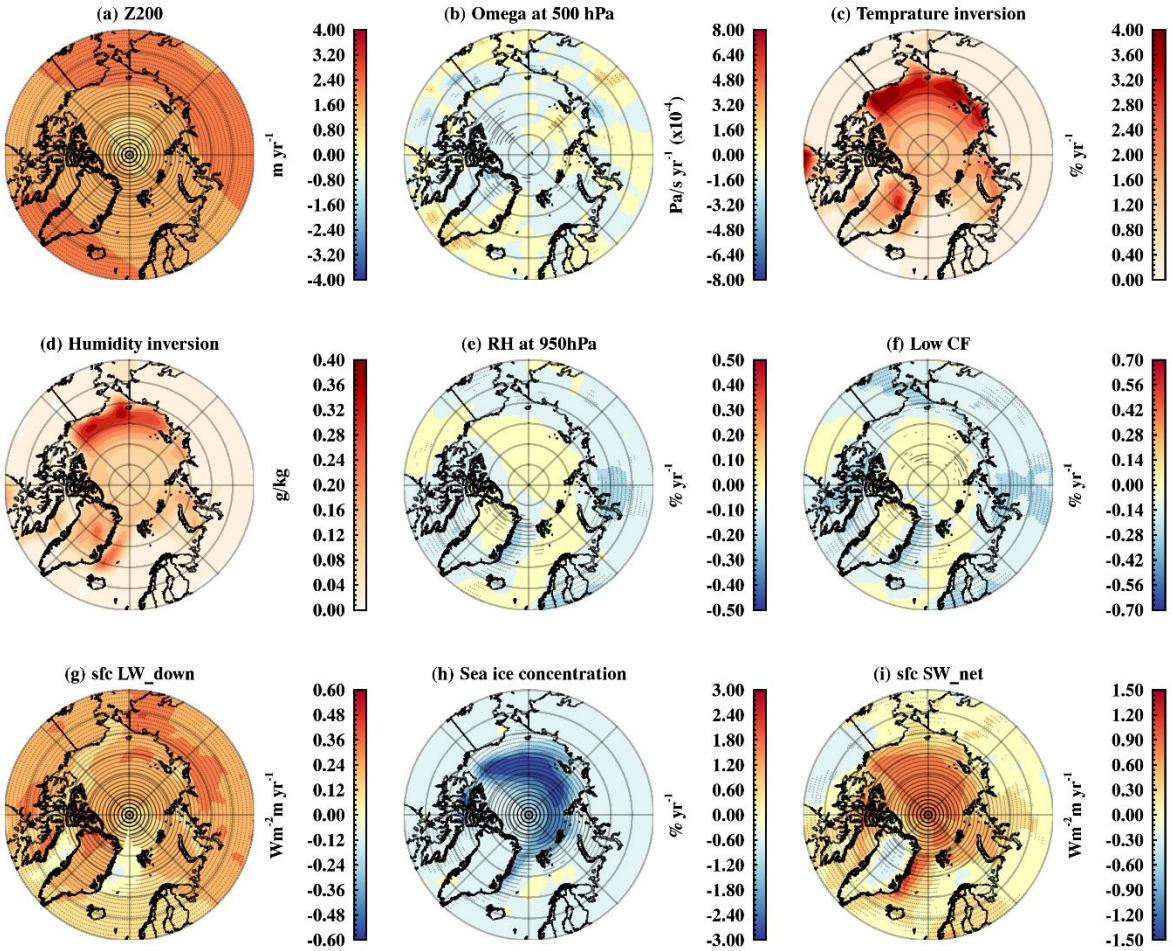

Supplementary Figure 7. Same as Figure 3, but using ensemble mean from CESM-LE RCP8.5 simulation during 2006-2022.

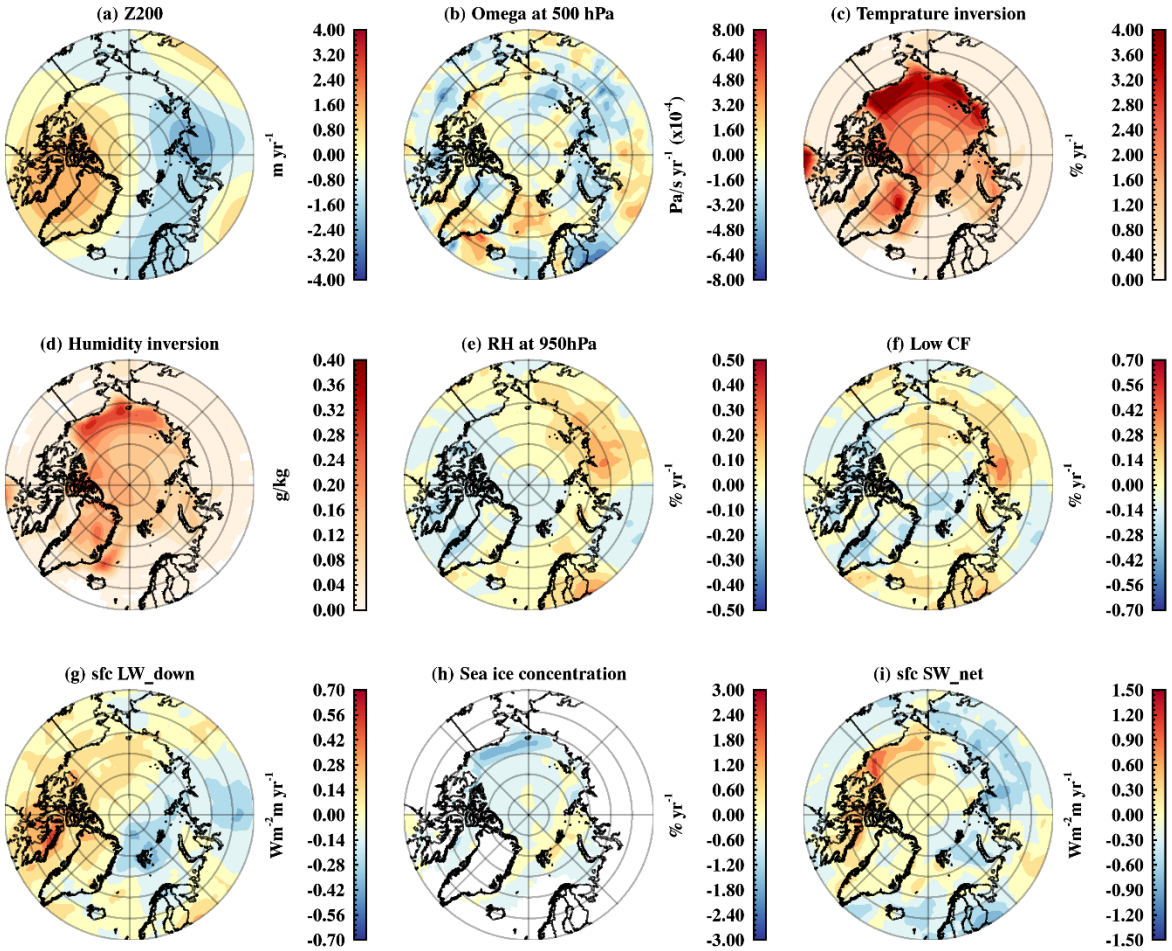

Supplementary Figure 8. Same as Figure 3, but using CESM-LE pre-industrial fully coupled simulation averaged from five selected non-overlapping 20-year episodes. These five pseudo-ensemble members exhibit the largest Z200 pattern correlations with ERA-Interim reanalysis.

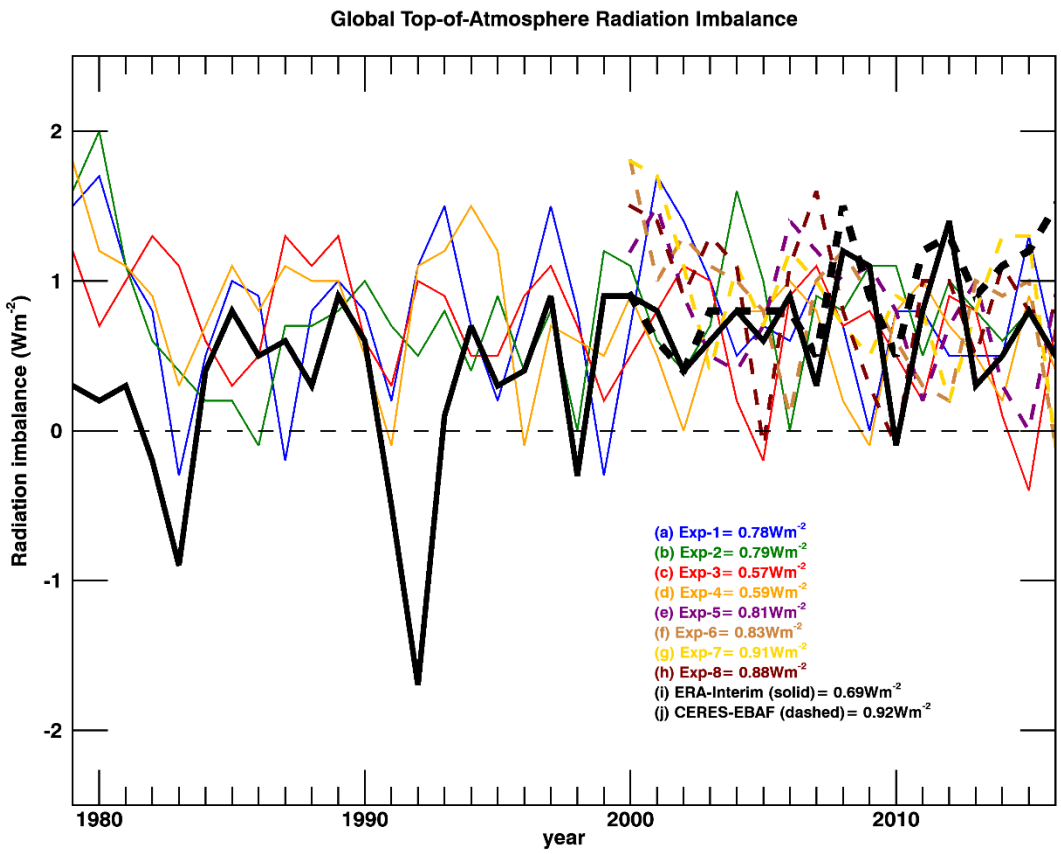

Supplementary Figure 9. The time series of global top-of-atmosphere radiation imbalance during 1979-2016. The colorful lines represent results from different CESM nudging experiments. The black solid line depicts results from ERA-Interim reanalysis, while black dashed line indicates results from CERES-EBAF Ed4.0 satellite product. The global weighted averages for radiation imbalance during 2000-2016 are provided for each simulation and dataset.

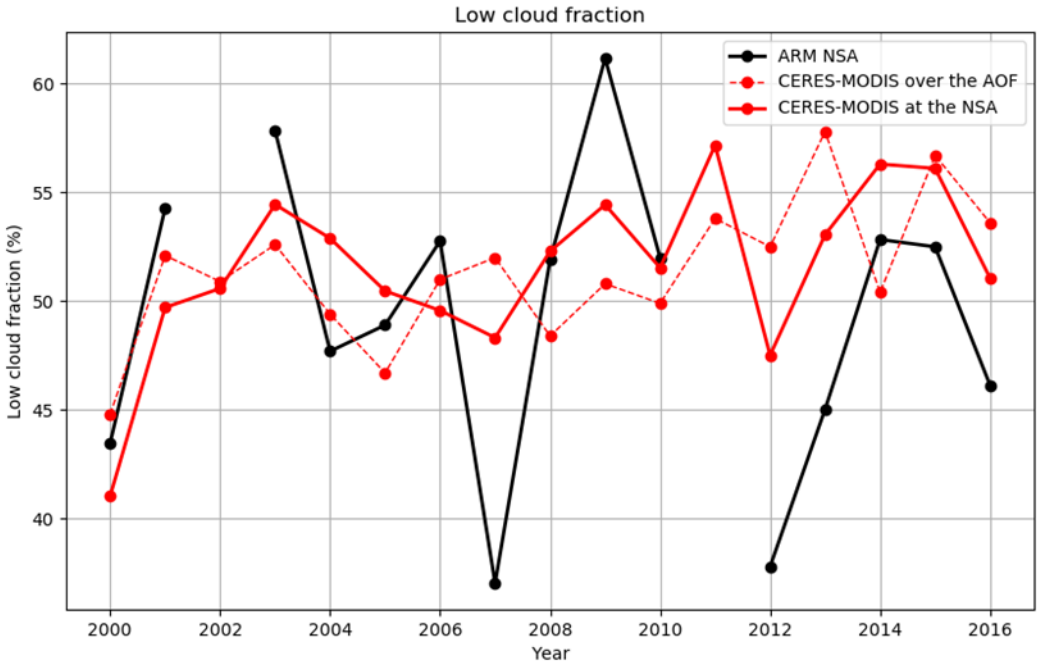

Supplementary Figure 10. The time series of low cloud fraction during 2000-2016. The black solid line represents results from surface in-situ measurements at Atmospheric Radiation Measurement (ARM) North Slope of Alaska (NSA, 71.33˚N -156.61˚) site. The red solid line depicts result from CERES SYN1deg Ed4.1 satellite product at NSA site, while the red dashed line indicates cloud fraction averaged over the area of focus (AOF, 71˚-80˚N, 162˚-222˚). The low clouds are defined as clouds below 700 hPa in CERES satellite product, while they represent clouds below 3 km in surface in-situ measurements. Note that the results from surface in-situ measurements during 2012-2016 are lower than those in 2000-2011 due to instrumental transitions.

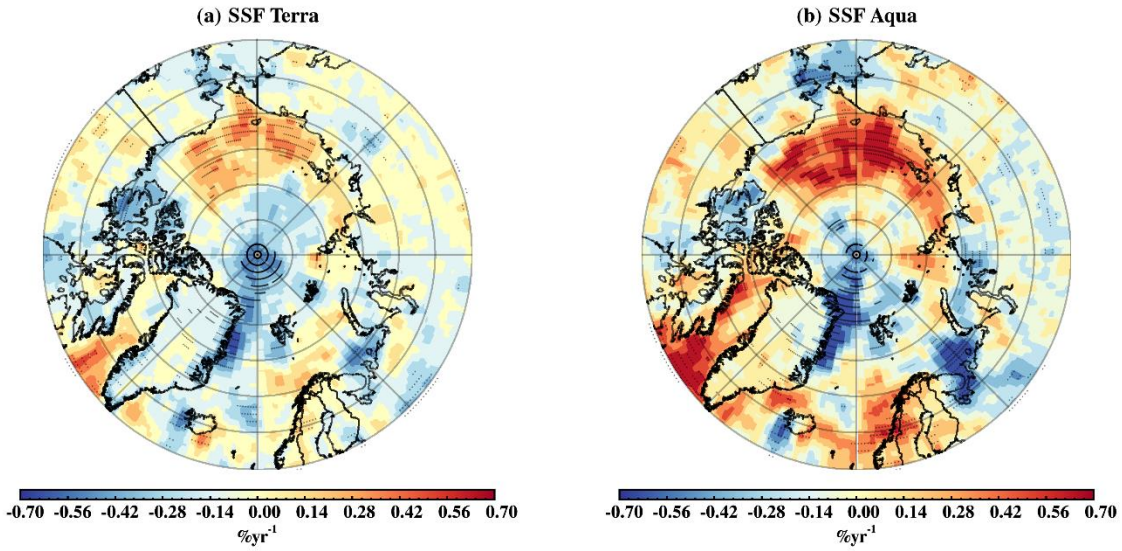

Supplementary Figure 11. The linear trend of low cloud fraction (below 700 hPa) in (a) NASA CERES-MODIS SSF1deg Terra Edition 4.1 (2000-2016) and (b) NASA CERES-MODIS SSF1deg Aqua Edition 4.1 (2002-2016).

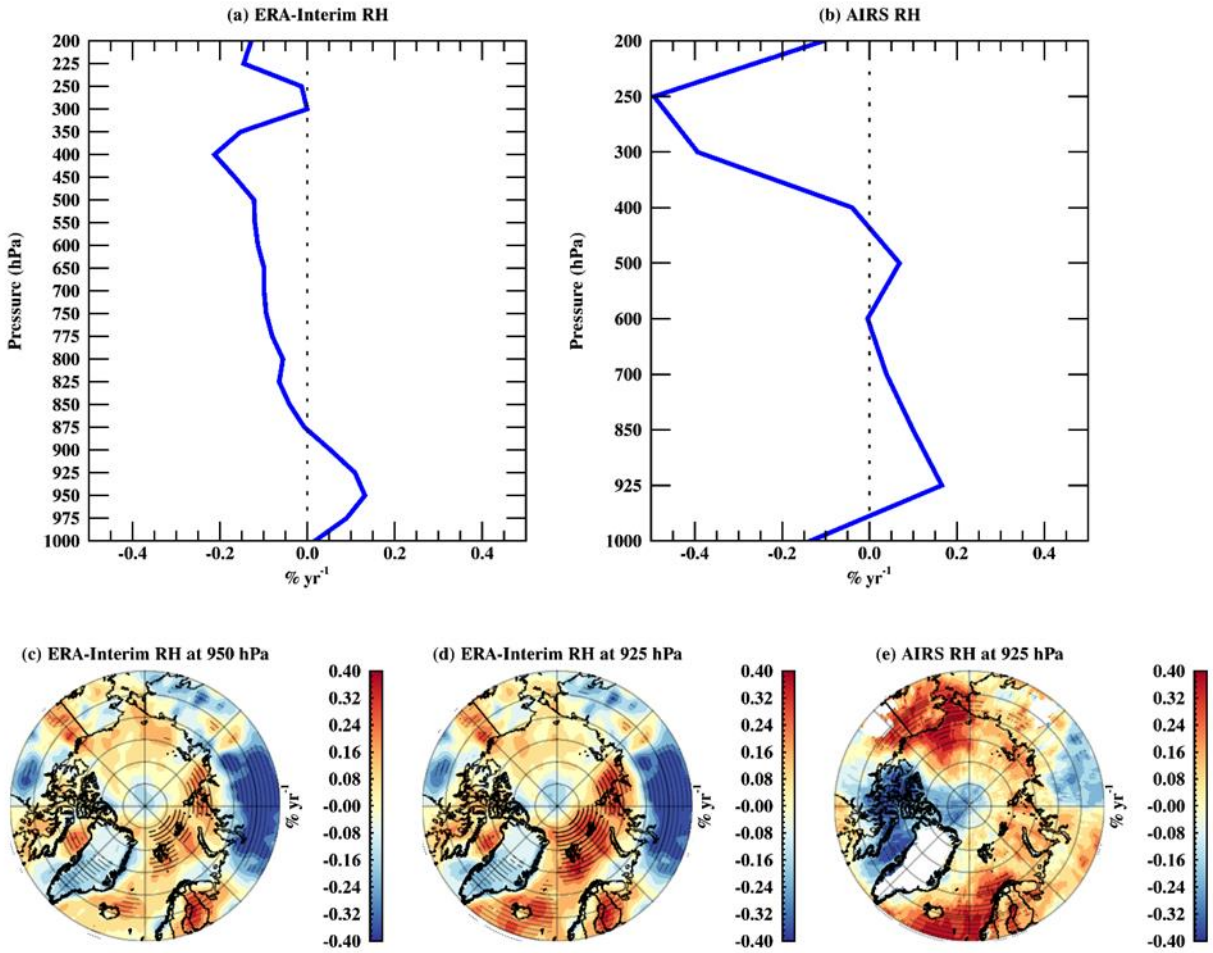

Supplementary Figure 12. Vertical structure of JJA relative humidity (RH) linear trend over the AOF (71˚-80˚N, 162˚-222˚) in (a) ERA-Interim reanalysis (2000-2016) and (b) NASA AIRS satellite product (2003-2016). The linear trend of (c) RH at 950 hPa and (d) RH at 925 hPa in ERA-Interim reanalysis and (e) RH at 925 hPa in AIRS satellite product.

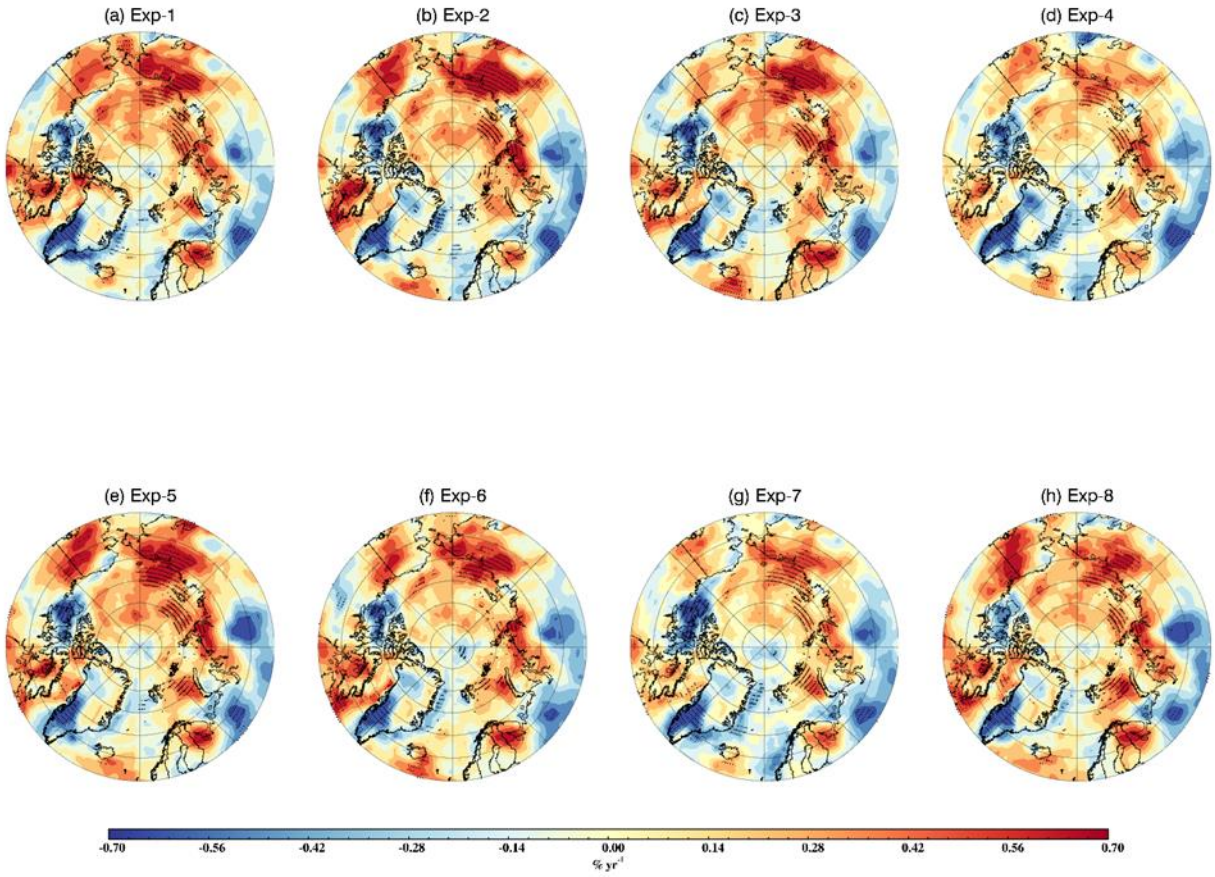

Supplementary Figure 13. The linear trend of JJA low cloud fraction (below 700 hPa) during 2000-2016 from eight sets of CESM nudging experiments.

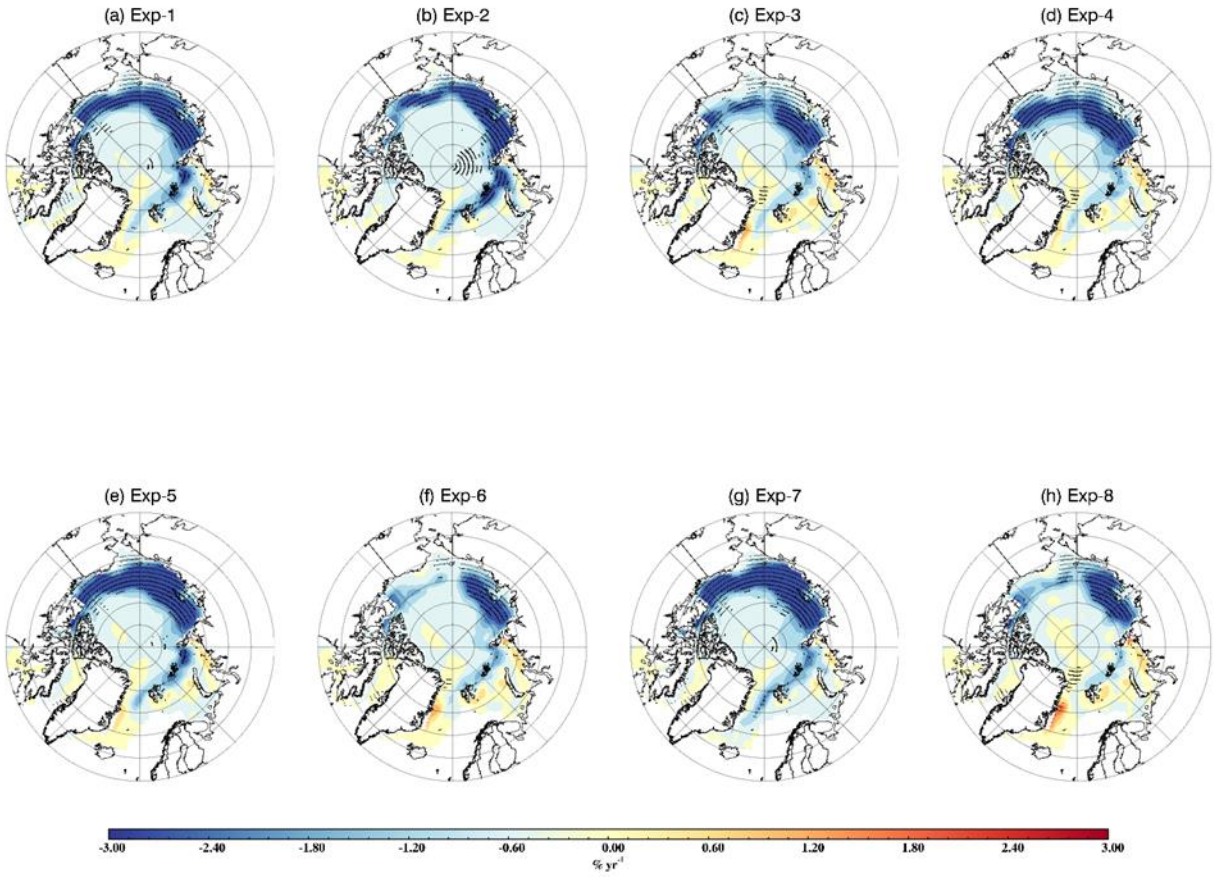

Supplementary Figure 14. Same as Supplementary Figure 13, but for September sea ice concentration.